TFAWS Thermal Control & Protection Paper Session

# Experimental Characterization of Additively Manufactured Nickel-Titanium Shape Memory Alloy Heat Pipes


William Sixel[1], Bilal Bomani[1]

[1]*NASA Glenn Research Center*

Tomé Seichi da Nóbrega Guenka[2], Christopher Greer[2]

[2]*The Pennsylvania State University*

Ryan Overdorff[3]

[3]*3D Systems*

Presented By

William Sixel



Thermal & Fluids Analysis Workshop
TFAWS 2026
August 31 – September 4, 2026
NASA Marshall Space Flight Center
Huntsville, AL

# Concept

## Passive Thermally Deployed Shape-Memory Alloy Heat-Pipe Radiators for High-Intensity Small Satellites

- Demonstrate additively manufactured (AM) NiTi radiators with integral wicking heat pipe networks.
- NiTi shape-memory alloy:
  foldable (origami) geometry that will passively deploy from stowed form
- Goals:
  - High deployed-to-stowed area ratio
  - Lower areal density
  - Low thermal resistance

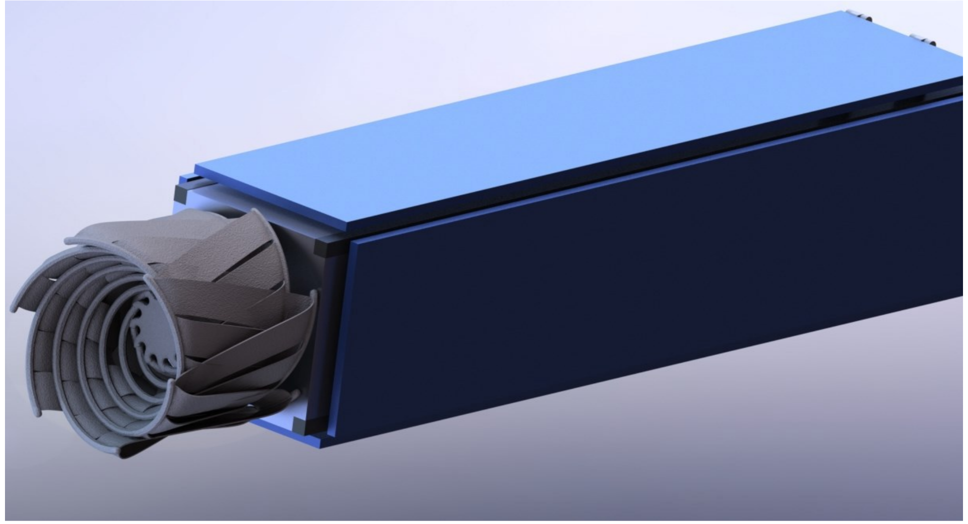

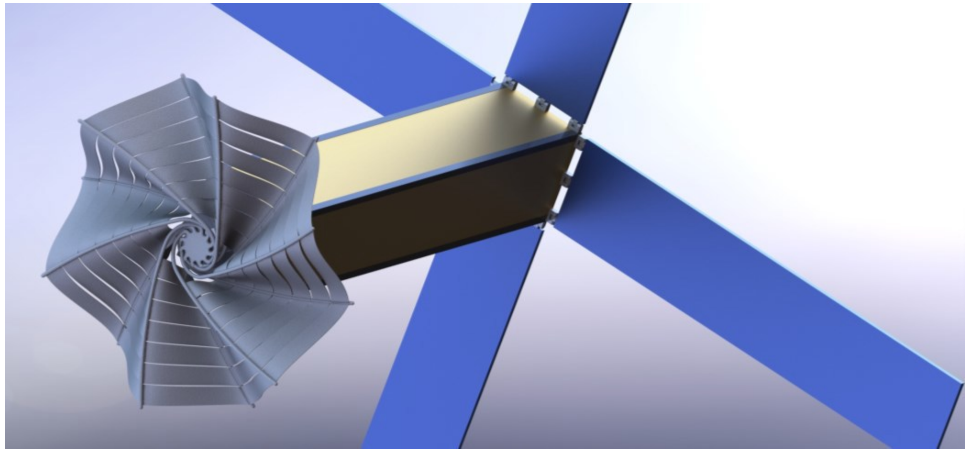

We wish to acknowledge generous support from NASA STMD through the Small Spacecraft Technology (SST) program (Grant 80NSSC23M0234).

# Bellows Heat Pipe Geometry

- Bellows heat pipe geometry is used to give greater flexibility for the heat pipe to allow for a greater ratio of stowed to deployed area.
- This comes at the cost of greater manufacturing complexity, and greater wick effective length (resulting in a lower capillary limit).
- Major goal of this test is to compare the bellows results to straight heat pipe results.

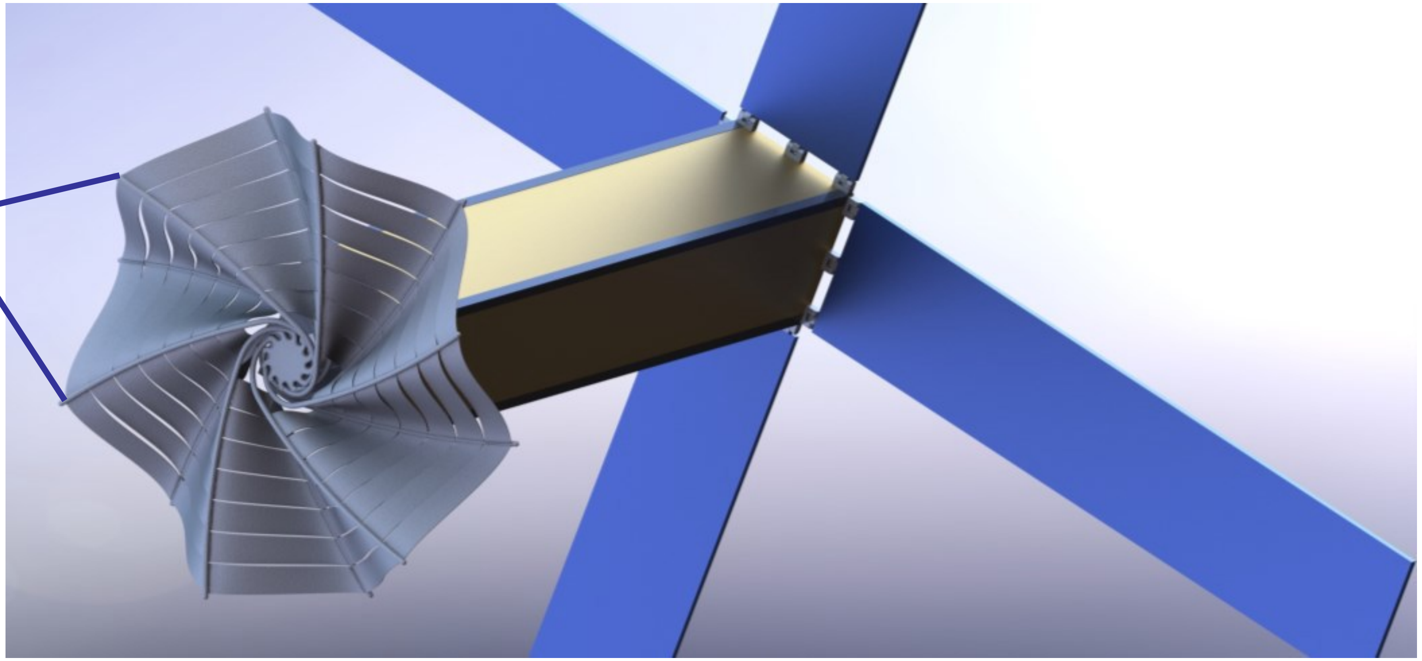

**Heat Pipes**

# Heat Pipe Manufacturing

- Coupons were fabricated through laser powder bed fusion (L-PBF)
  - Fort Wayne Metals atomized NiTi #5, 3D Systems DMP Flex 100 metal 3D printer
- Powder has 55.1 wt% Ni and 45 µm median particle size
  - Expected $A_f$ (austenite finish) temperature of 358 K.
- Integral wicks printed using the rastering strategy described in Guenka et al., 2024
  - Hatch distance of 400 µm.
  - 75 % of the laser power used for the dense parts.
  - Layer scan orientation rotation every 3 layers.

**Top view of two different hatch spacing wicks (build direction out of screen)**

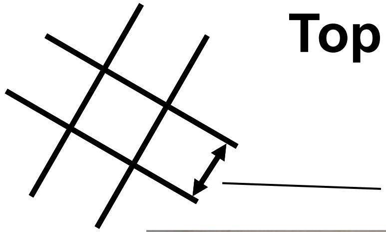

**275 µm** **400 µm**

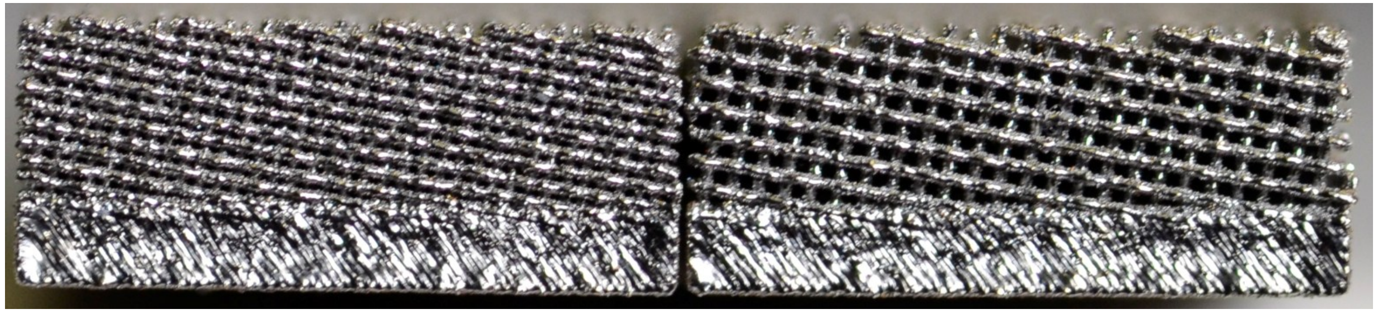

**Side view of 400 hatch spacing wick (rotated every 6 layers)**

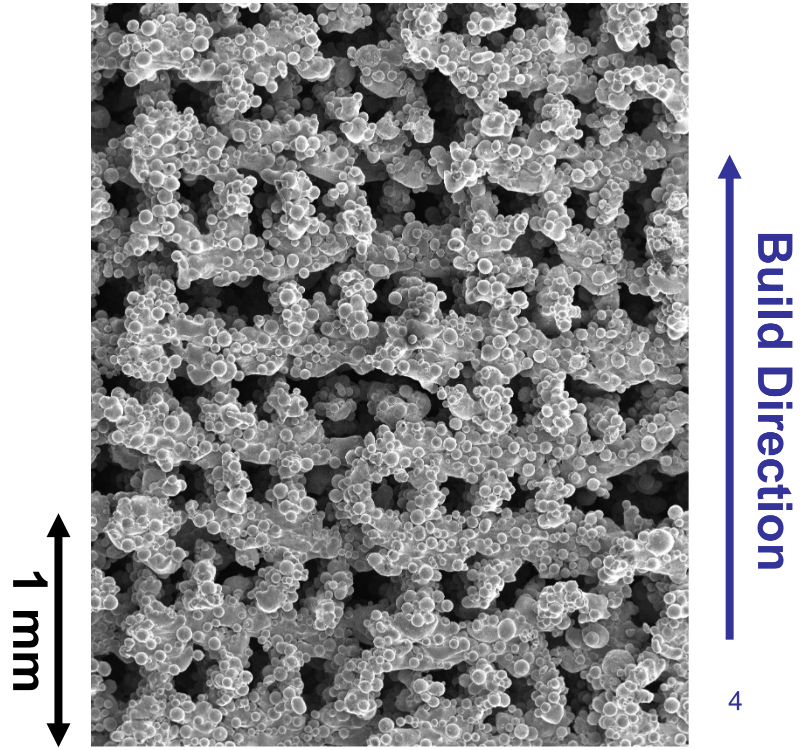


*Guenka et al. "Additive Manufacturing and Experimental Characterization of Nickel-Titanium Shape-Memory Alloy Wick Structures and Heat Pipes for Spacecraft Thermal Control.", TFAWS 2024.*

# Heat Pipe Manufacturing

- Before & after removal from the build plate

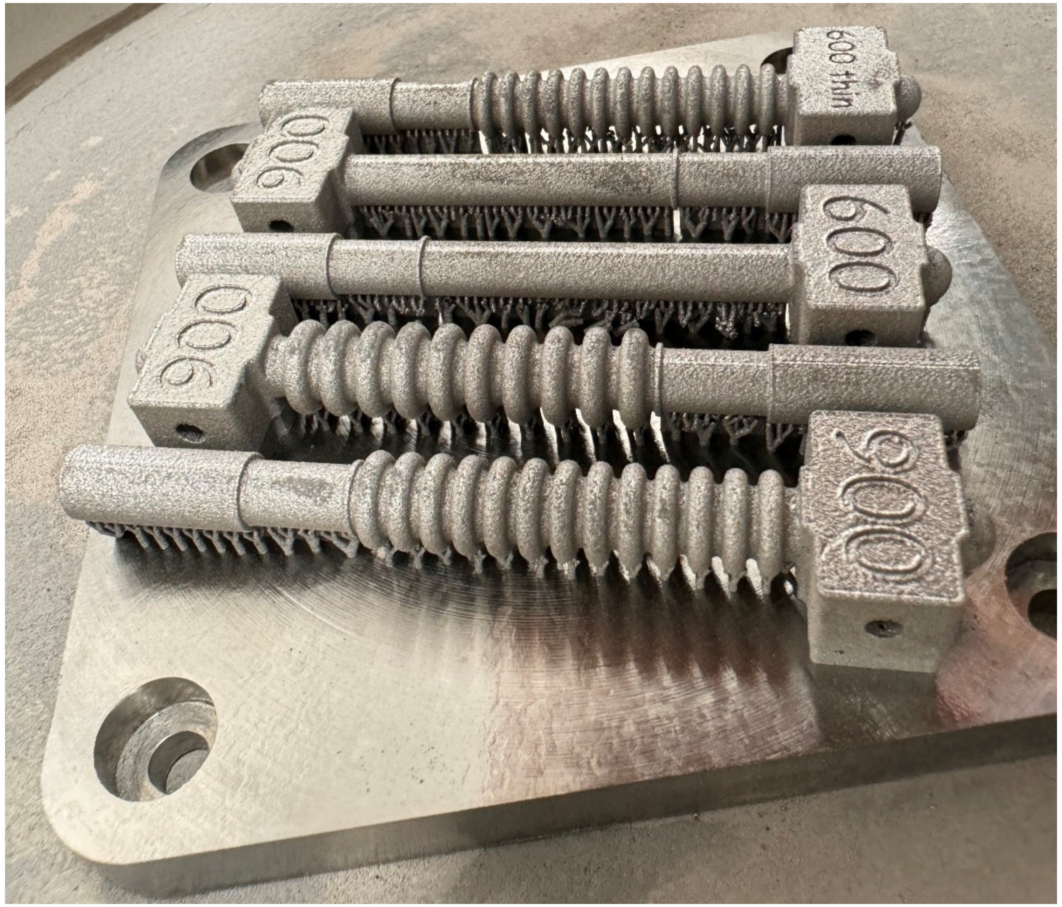


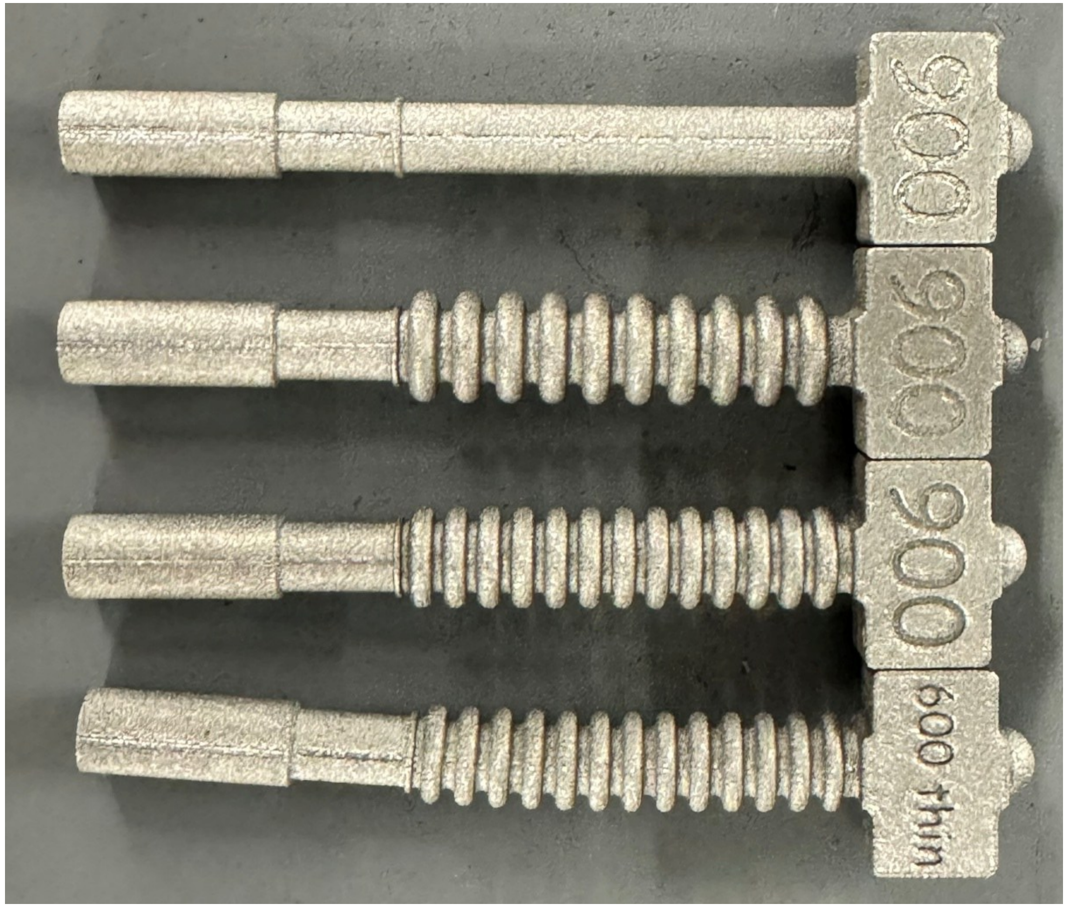

# Test Configuration

- Post machining for threads, evaporator interface, & compression fitting
- Test setup shown left prior to adding insulation & condenser coolant lines.

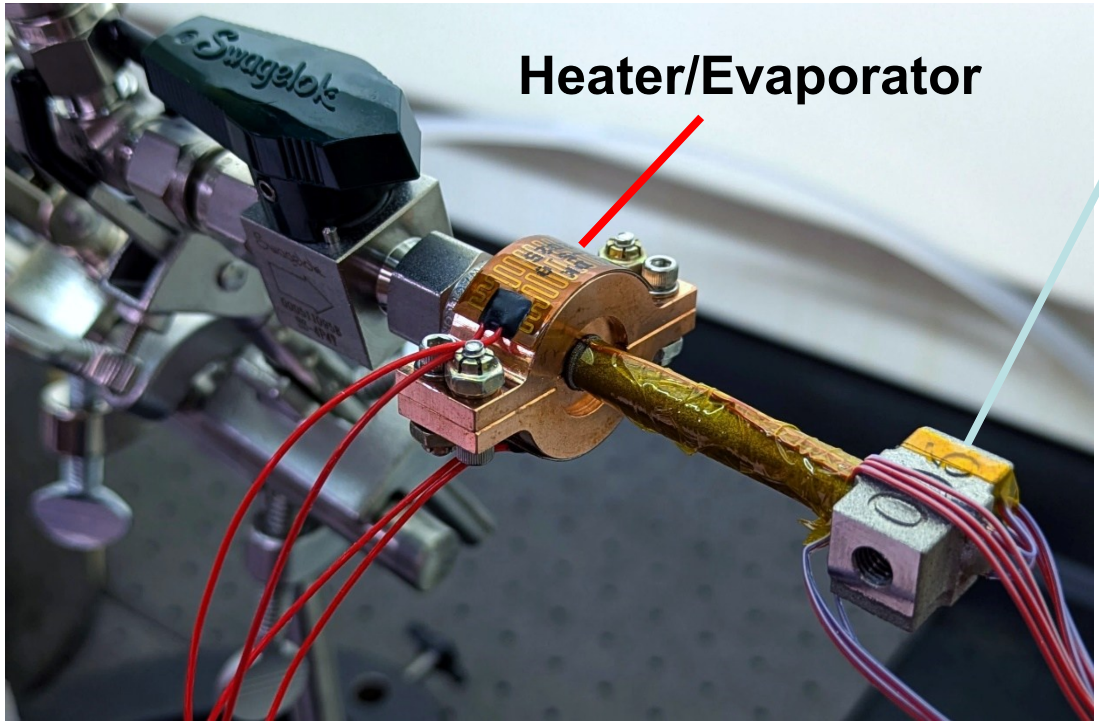


Straight heat pipe sample

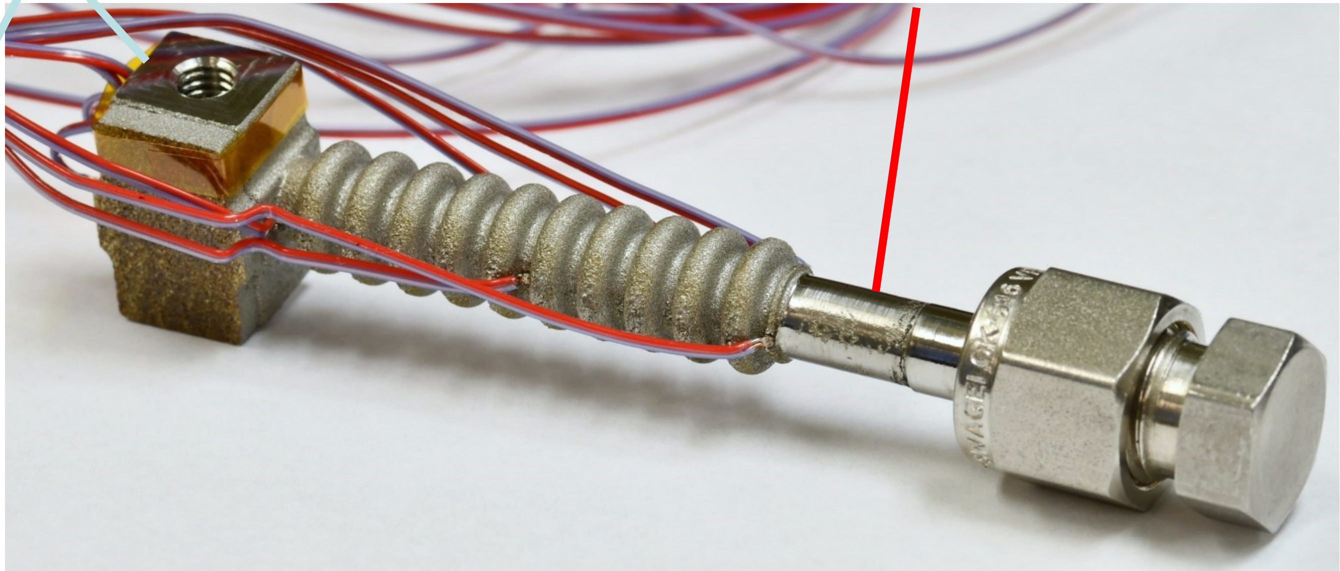


Bellows heat pipe sample

# Instrumentation

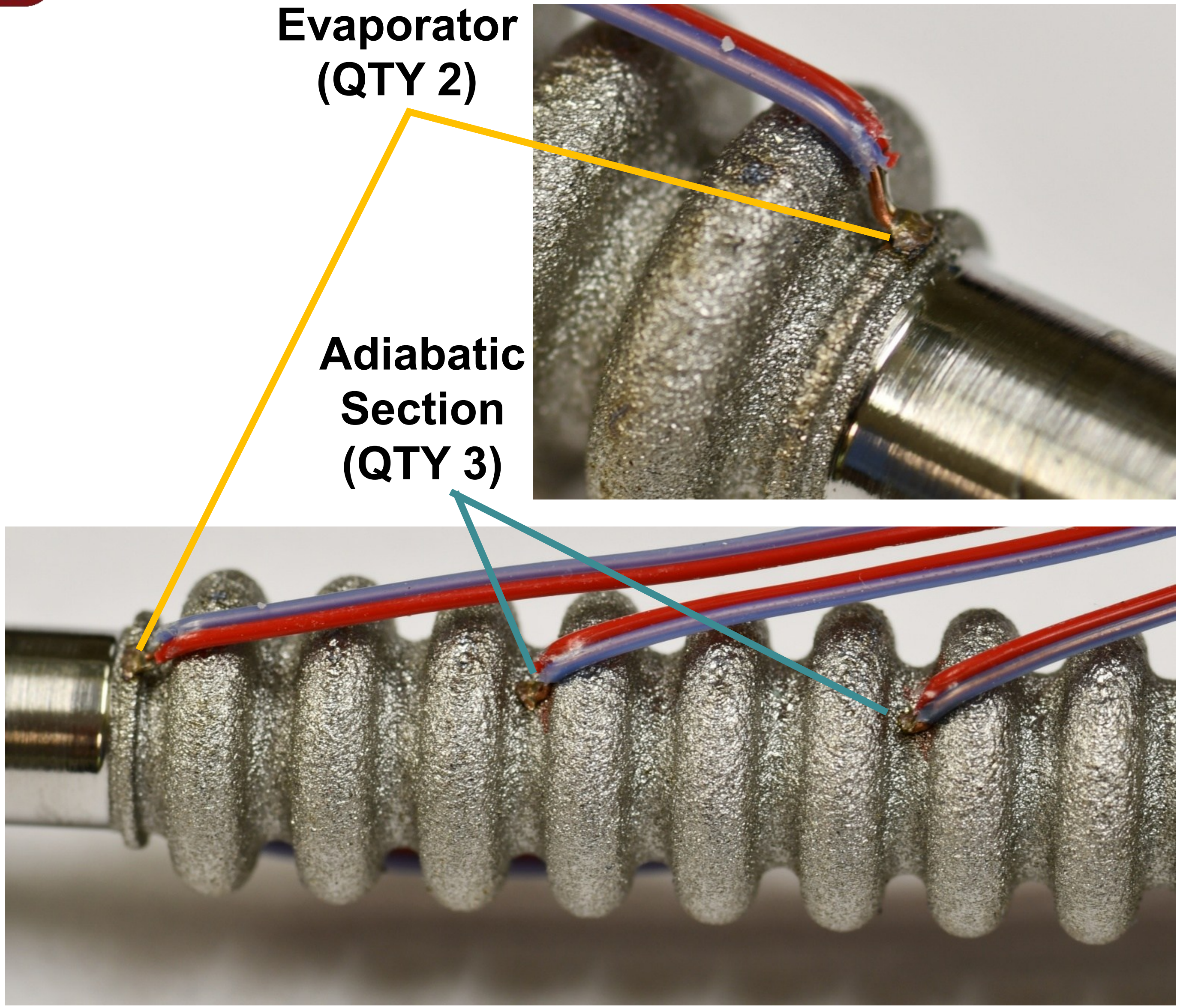



***All PFA Insulated 30 AWG Type T Thermocouples***

# Heat Leak & Contact Resistance Corrections

- Tested heat pipes dry to quantify the heat leak to ambient.
  - Conduction + Leak through insulation
  - Total resistance to ambient: 24-30 K/W
  - Use this to correct the actual heat load into the heat pipe.
- Estimated thermal contact coefficient
  - Estimated by the difference between the saddle temperature measurement and the evaporator TC.
  - Max and min values given by:
    - The unmodified heat load (assuming all heat leak happens by conduction), or
    - Adjusted heat load (all heat leak directly from heater through insulation to ambient).
  - Use this contact coefficient to correct the evaporator temperature measurement.

$$R_{leak} = \frac{T_{evap} - T_{ambient}}{\dot{q}}$$

$$h_{contact} = \frac{\dot{q}''_{evap}}{T_{heater} - T_{evap}}$$

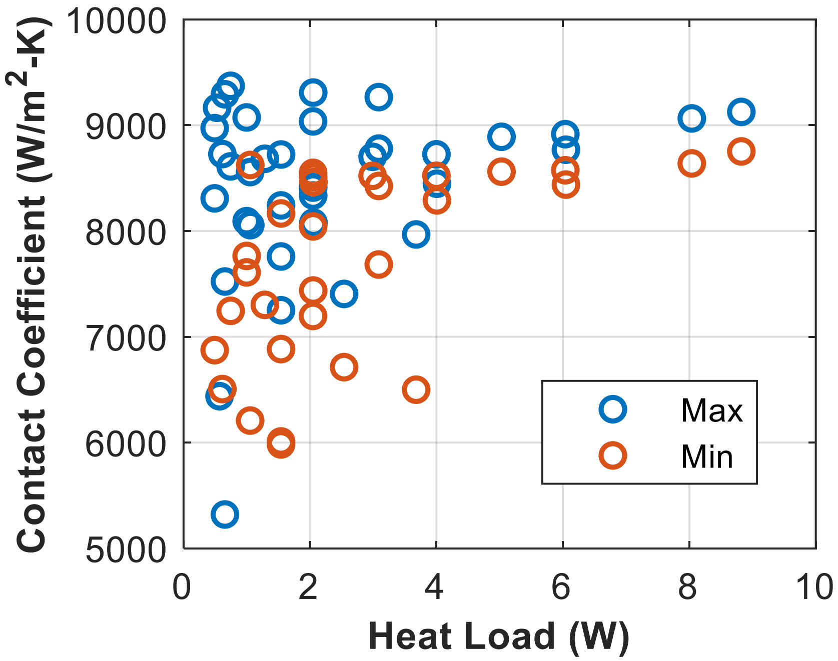

# Initial Test Results

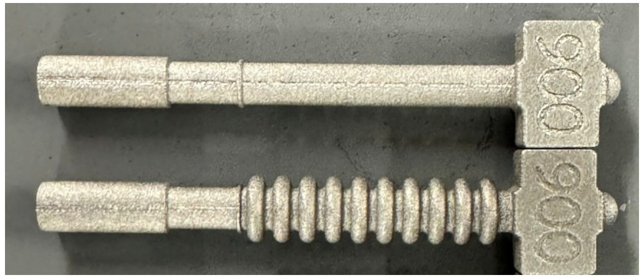


- Three heat pipe samples
  - Straight heat pipe with 0.9 mm thick wick
  - Straight heat pipe with 0.6 mm thick wick
  - Bellows heat pipe with 0.9 mm thick wick
- Observed in initial testing that with the observed large evaporator ΔT, that all tests would be limited by boiling, not by the capillary limit.
  - Attempted to observe the capillary limit by changing orientation with respect to gravity.
  - This proved ambiguous, as it also changed the conductance and appeared to just reach the boiling limit at a lower heat load.
  - *Realized that the 0.6 mm wick sample would give the best data, as it would be able to reach a higher heat load as it theoretically has a lower conductance due to thinner wick.*
  - Focused testing on 0.6 mm wick to understand wick behavior best.

# Normalization

- Can plot T vs x directly, or …
- Can also normalize for each run by calculating:

$$t_{norm} = \frac{T(x) - T_{condenser}}{T_{heater} - T_{condenser}}$$

  – This produces a temperature value from 0 to 1 for **each** pipe (each steady state point is normalized to itself).
- For an ideal constant conductance heat pipe, we would expect this to collapse every data point (for a working fluid) onto a single line.
  – However, variances in test quality, and changes in test variables (fluid, charge mass, and even heat load) will change the shape of the curve.

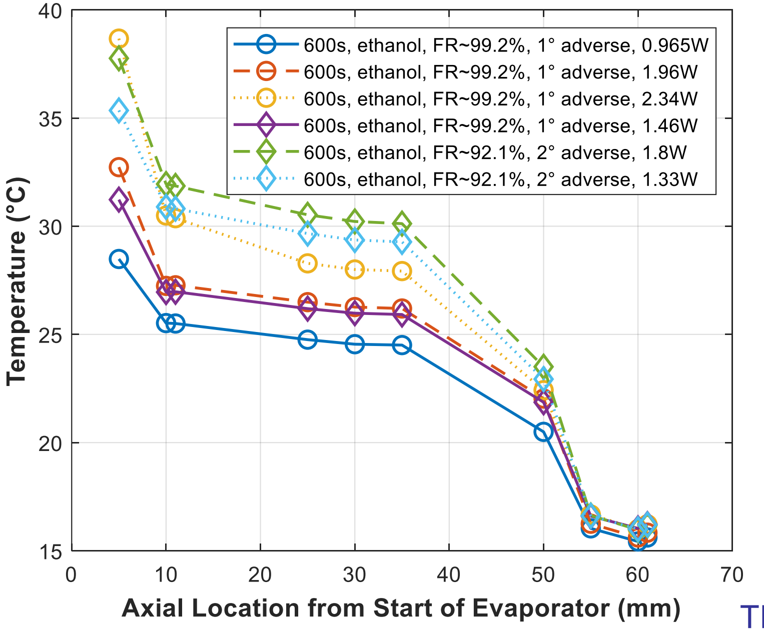


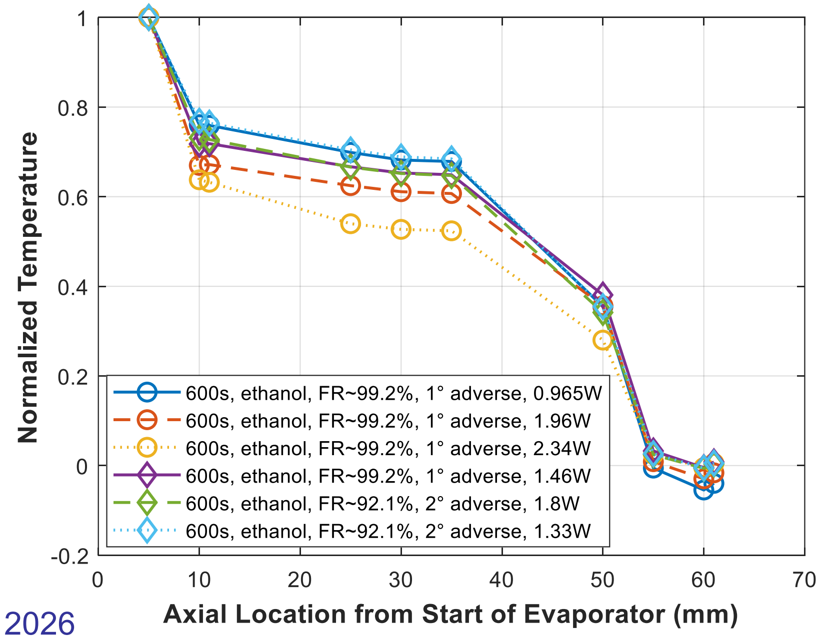

# Broad Test Results

- All test results show the overall expected behavior for a heat pipe:
  - Approximately constant axial temperature in the adiabatic section.
  - Large local temperature drops in the evaporator and condenser sections.
    - Due to wall/wick heat transfer
  - Indicative of a correctly functioning heat pipe with heat transfer due to capillary flow relative to just the axial conduction.
  - Two dry cases are shown.
    - Show the expected linear temperature profile.
- The relative temperature drop varies…
  - Evaporator vs condenser thermal resistance.
  - Changes based on:
    - Working fluid
    - Heat load

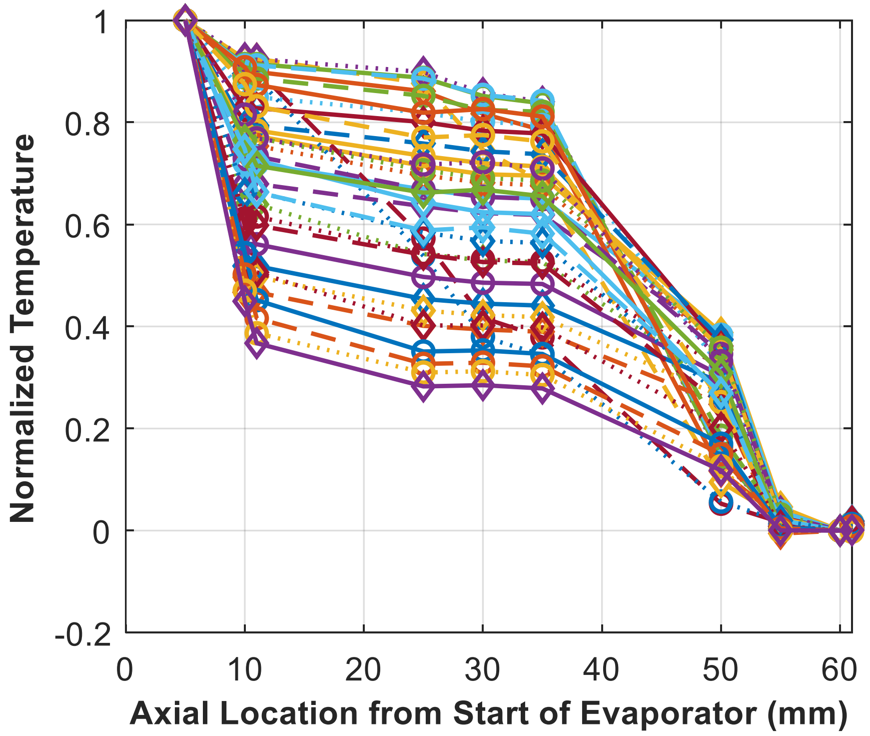

# Apparent Thermal Resistance of the Heat Pipes

- Heat pipe thermal resistance plotted for all heat loads & working fluids.
- Most notable trend:
  - Evaporator thermal resistances tends to approach a constant as heat load exceeds 1 W.
  - Condenser resistance tends to continuously decrease with increasing heat load.
  - Likely related to fluid distribution within the heat pipe.

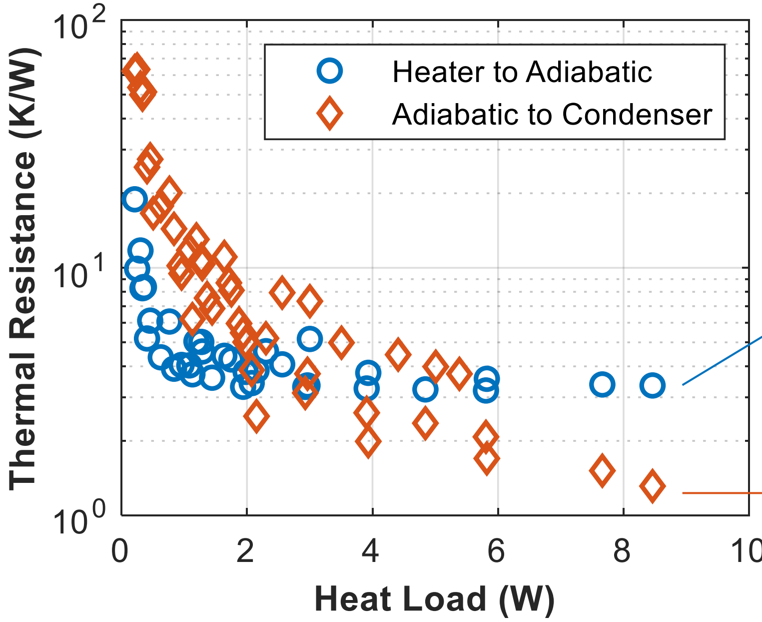


$$R_{evap} = \frac{T_{heater} - T_{sat}}{\dot{q}_{corrected}}$$

$$R_{cond} = \frac{T_{sat} - T_{cond}}{\dot{q}_{corrected}}$$

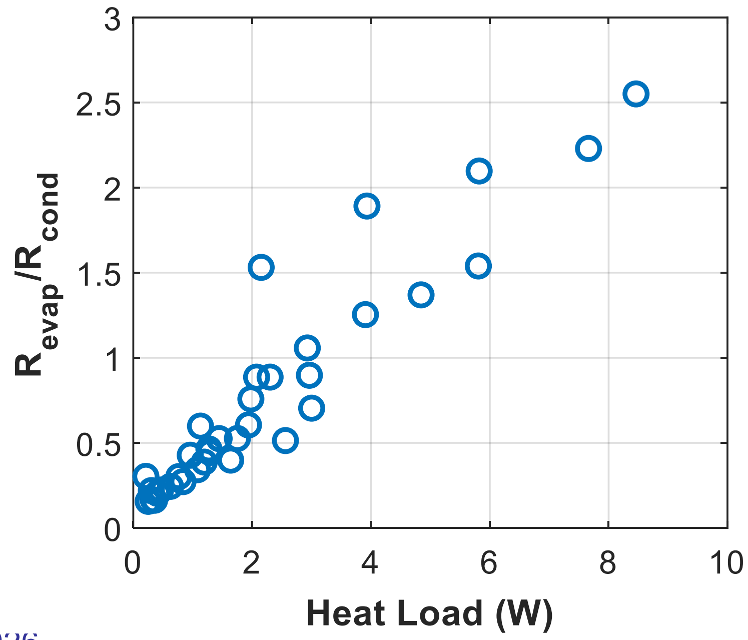

# AM Wick Effective Thermal Conductivity

- The effective thermal conductivity of the wick can be calculated after correcting for other thermal resistances:
  - Total resistance $R_{evap}$ is measured.
  - Copper saddle and heat pipe wall conductivities are calculated for known conductivity and geometry.
  - Contact resistance is calculated with the observed ~10,000 W/m$^2$-K contact coefficient.
- Compared to a simple screen wick conductivity correlation (Alexander).

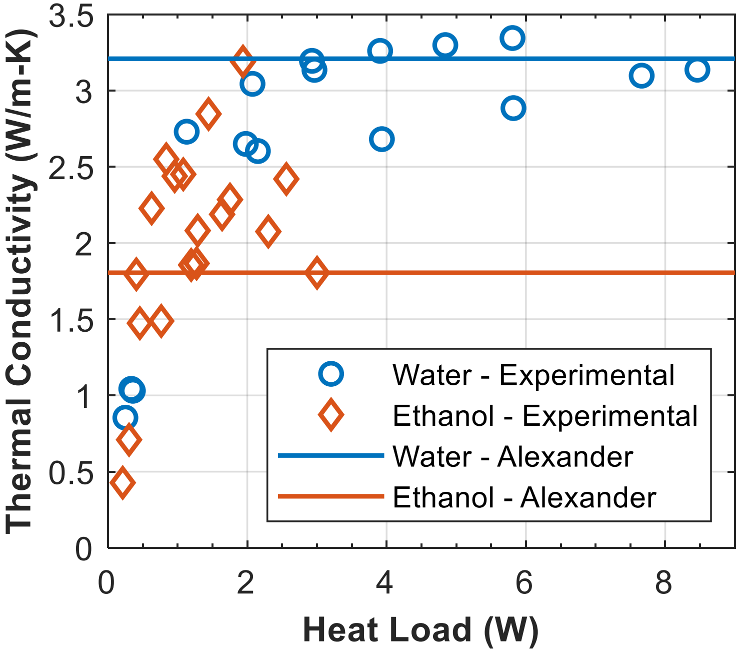


$$R_{evap,wick} = R_{evap} - (R_{saddle} + R_{contact} + R_{wall})$$

$$k_{eff} = \frac{\ln(OD_{wick}/ID_{wick})}{2\pi L_{evap} R_{evap,wick}}$$

$$k_{Alexander} = k_f \left(\frac{k_s}{k_f}\right)^{1-\beta^{.59}}$$

*Alexander, E. G. "Structure-Property Relationships in Heat Pipe Wicking Materials." Ph.D. Thesis, North Carolina State University, 1972.*

# Bellows Heat Pipe Test Results

- Tested with ethanol and water in slight gravity adverse condition.
  - In both cases, reached higher heat loads than previous tests.
  - Probably partially due to optimized charge ratio & procedure, as test campaign progressed.

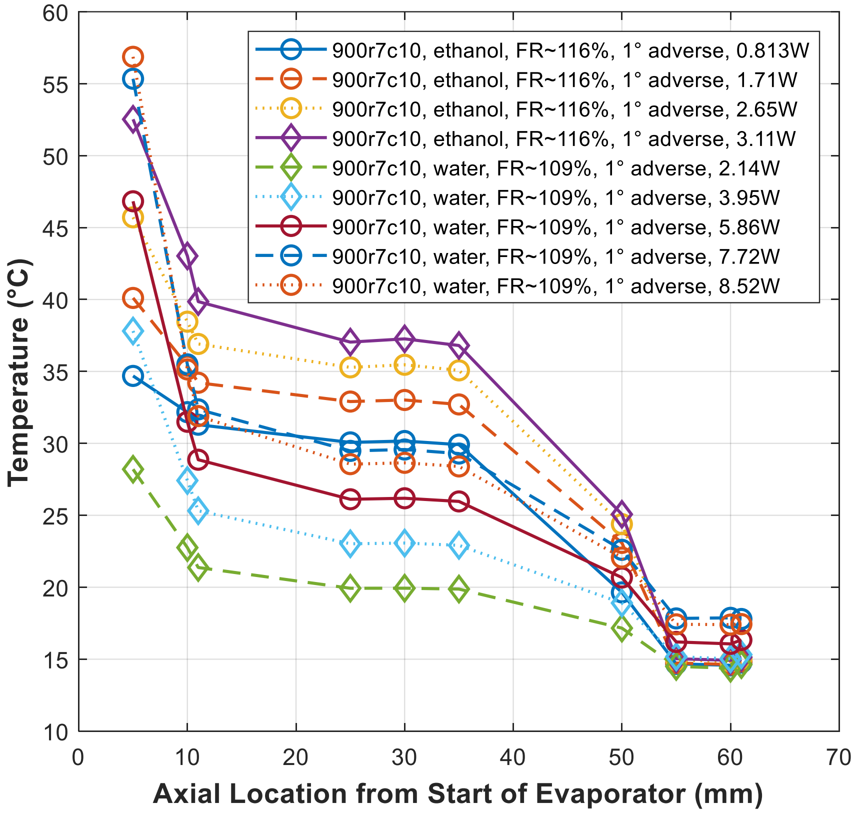


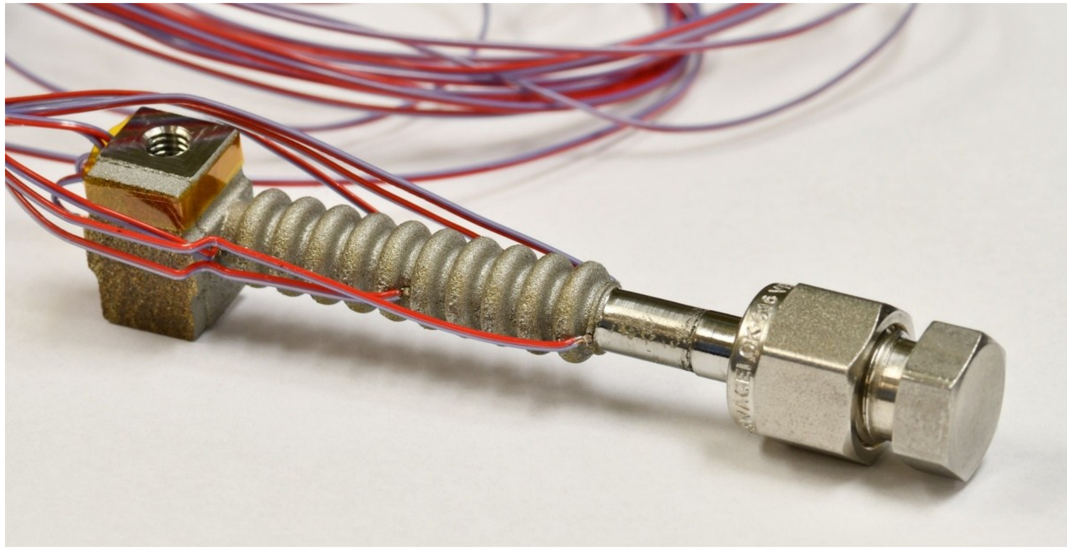

# Bellows Heat Pipe Thermal Resistance

- Initial testing with 0.9 mm heat pipe did not have heater thermocouple.
  - Only measured evaporator temperature on the heat pipe.
  - Added separate heater temperature measurement for 0.6 mm heat pipe test.
  - As a result, compared 0.9 mm thick bellows heat pipe to 0.6 mm straight heat pipe.
- Straight vs Bellows Comparison
  - Expect straight (thinner wick) coupon to perform better
    - Shorter wicking length
    - Thinner wick == less thermal resistance.
    - Should not reach capillary limit for either wick.
  - Ethanol Result:
    - Bellows result reached **higher** heat load (unexpected).
      - At slightly higher resistance (expected).
  - Water Result:
    - **Lower** or same thermal resistance
    - **Higher** heat load (unexpected).

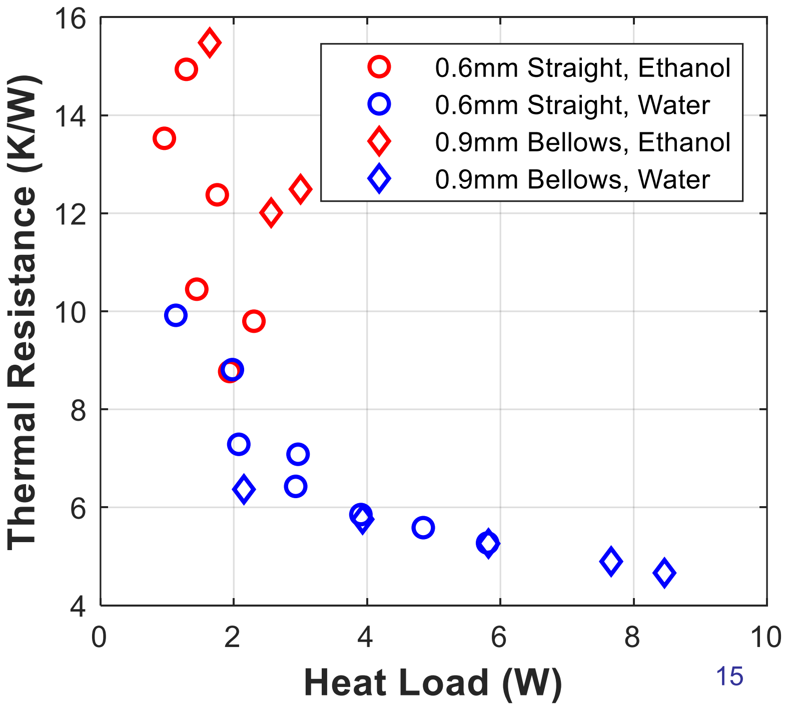

# Evaporator Performance

- Superheat is calculated from the measured ΔT and corrected to only include the component from the wick.
- Observe that these heat pipes with water can tolerate much higher superheat than with ethanol (expected from literature).
- Results with water are linear up to the apparent stability limit.
  - Attempted higher heat loads.
    - Could not reach steady state.
- Ethanol results nonlinear
  - This is the onset of nucleate boiling in the wick.
    - Partial dryout
  - Trend bifurcates around 5-10 K of superheat.

$$\Delta T_{superheat} = \dot{q} R_{evap,wick}$$

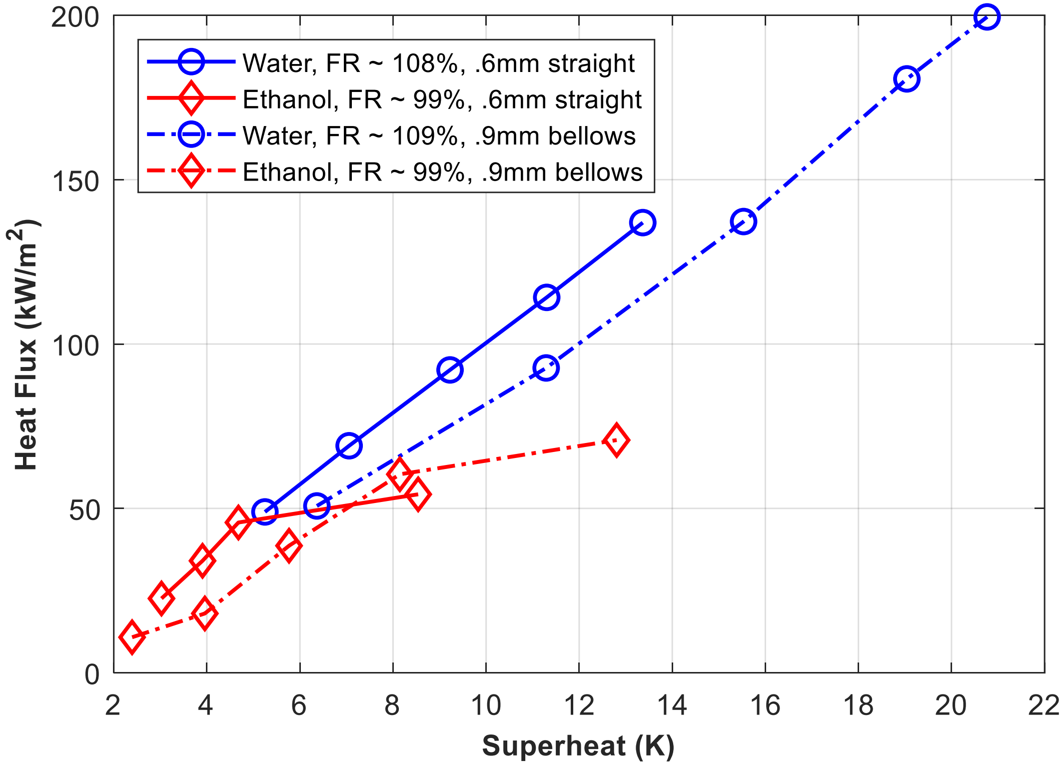

# Conclusions

- Could not reach a conclusive capillary limit in testing; downside of current coupons.
  - Have K/r data from previous rate-of-rise testing to inform this design in the future.
  - Thinner wicks difficult to achieve due to printing limitations.
  - Future designs may need larger evaporator.
- Bellows heat pipe reached higher heat load in the bellows heat pipe than in any previous test.
  - Not necessarily expected:
    - Bellows geometry significantly more difficult to produce a high-quality wick print.
    - Bellows has a longer effective length for wicking.
  - Confirms, at least:
    - Capillary limit is not dominant in tested designs; rather the boiling limit.
    - If capillary limit was lower than boiling limit, would observe lower heat load limit in bellows.
    - **AM Bellows geometry achievable for future demo!**
      - **At least these samples, bellows geometry does not dominate performance.**

# Questions?